Determination of Quadrupole Transition Amplitudes by Polarized-Deuteron Scattering

H. Clement, R. Frick, G. Graw, F. Merz, P. Schiemenz, N. Seichert, and Sun Tsu Hsun[(a)]
Sektion Physik, Universität München, D-8046 Garching, Germany
(Received 15 May 1980)

The inelastic scattering of 20-MeV vector-polarized deuterons from ^{24}Mg, ^{28}Si, ^{32}S, and ^{54}Cr provides an experimental determination of sign and magnitude of the quadrupole mass transition amplitudes $\langle 2_1^+\|Q^m\|2_1^+\rangle$, $\langle 2_2^+\|Q^m\|2_2^+\rangle$, and $\langle 0_1^+\|Q^m\|2_2^+\rangle\langle 2_2^+\|Q^m\|2_1^+\rangle\langle 2_1^+\| \times |Q^m\|0_1^+\rangle$, which correspond to the static quadrupole moments $Q_{2_1^+}$ and $Q_{2_2^+}$ and the P_3 interference term in the case of electromagnetic transitions.

PACS numbers: 23.20.Js, 24.70.+s, 25.50.Dt

For the spectroscopy of low-lying states of even-even nuclei it is fundamental to experimentally determine all transition amplitudes. Of special importance are the quadrupole transition amplitudes connecting the 0_1^+ ground state and the two low-lying 2^+ states, which are indicated in Fig. 1 and labeled as $\langle 1\rangle$ to $\langle 5\rangle$. In electromagnetic processes the absolute magnitudes of the dynamic charge transitions $\langle 1\rangle^c = \langle 2_1^+\|Q^c\|0_1^+\rangle$, $\langle 3\rangle^c = \langle 2_2^+\|Q^c\|2_1^+\rangle$, and $\langle 5\rangle^c = \langle 2_2^+\|Q^c\|0_1^+\rangle$ have been obtained from Coulomb excitations and measurements of lifetimes, branching ratios, and mixing ratios. The aim of more recent investigations has been the determination of sign and magnitude of the static charge quadrupole moment $Q_{2_1^+}$ in the 2_1^+ state via the observation of the reorientation effect in Coulomb excitation. The determination of this quantity is based on the observation of an interference between a one-step and a two-step process: the direct excitation $\langle 1\rangle$ of the 2_1^+ state and the same excitation followed by reorientation $\langle 1\rangle\langle 2\rangle$. The 2_1^+ excitation is affected furthermore by transitions via other levels, predominantly the 2_2^+ level. This two-step transition $\langle 3\rangle\langle 5\rangle$ causes in the 2_1^+ scattering another interference with the direct excitation $\langle 1\rangle$ called

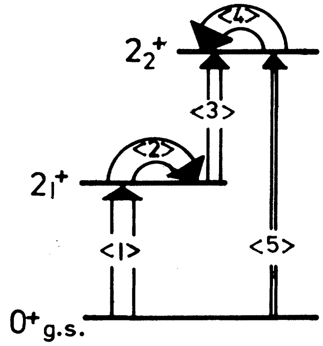

FIG. 1. Quadrupole transitions $\langle f\|Q\|i\rangle$ between the states 0_1^+, 2_1^+, and 2_2^+.

$P_3 = \langle 1\rangle^c\langle 3\rangle^c\langle 5\rangle^c$. It is a measure of the degree of mixing between the two 2^+ states; in a collective picture its sign relative to $Q_{2_1^+}$ reflects the presence of either the γ or β degree of freedom. For further implications we refer to the recent discussion on ^{194}Pt by Baker[1] and references therein. Contrary to the numerous measurements[2] of $Q_{2_1^+}$, the sign of P_3 has been determined so far only in very few instances. In this Letter, we show that the scattering data of 20-MeV vector-polarized deuterons depend in a characteristic way on the quadrupole mass transition amplitudes $\langle 1\rangle^m$ to $\langle 5\rangle^m$. A coupled-channels analysis of our data for ^{24}Mg, ^{28}Si, ^{32}S, and ^{54}Cr provides the absolute magnitudes of $\langle 1\rangle^m$, $\langle 2\rangle^m$, $\langle 3\rangle^m$, and $\langle 5\rangle^m$, and qualitatively of $\langle 4\rangle^m$, as well as a determination of the signs of $\langle 2\rangle^m \sim Q_{2_1^+}$, $\langle 4\rangle^m \sim Q_{2_2^+}$, and $\langle 1\rangle^m\langle 3\rangle^m\langle 5\rangle^m \sim P_3$.

The experiments have been performed with the polarized deuteron beam of the Munich MP tandem accelerator. Details are described elsewhere.[3] A large number of transitions have been analyzed; Fig. 2 shows cross section $\sigma(\theta)$ and vector analyzing power $iT_{11}(\theta)$ for the excitation of the two lowest 2^+ states.[4] Both $\sigma(\theta)$ and $iT_{11}(\theta)$ exhibit pronounced differences between the 2_1^+ and 2_2^+ transitions, which indicate the presence of strong and distinctive two-step processes interfering with the direct excitations. In view of the reaction picture noted above, these interferences are due to the existence of the quadrupole moments in each of the 2^+ states and of the P_3 term.

The curves in Fig. 2 are results of coupled-channels (CC) calculations with use of the code ECIS.[5] The actual calculations also include other excited states (4^+, etc.). Their influence on the 2^+ scattering, however, is rather weak and can be neglected for the further discussion. In all cases a reasonable reproduction of the data was achieved by the CC analyses performed in the parametrization of a collective-model *Ansatz*. For the spherical part of the deuteron-nucleus inter-

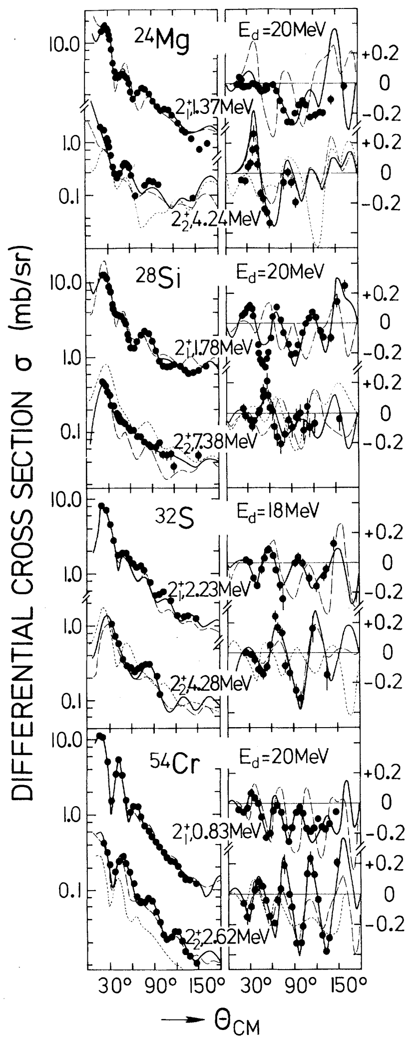

FIG. 2. Vector analyzing power $iT_{11}(\theta)$ and differential cross section $\sigma(\theta)$ for the 2_1^+ and 2_2^+ states in ^{24}Mg, ^{28}Si, ^{32}S, and ^{54}Cr. The drawn curves are explained in the text.

action we have used a global set of optical-model parameters, which resemble closely those of Ref. 6. (Other global sets have been found to give essentially the same results.) The deformed part of the deuteron-nucleus interaction is determined by the reduced matrix elements $\langle 1\rangle^m$ to $\langle 5\rangle^m$, which contain the nuclear structure information, and the radial form factors, which are taken to be of collective type.[7] It is believed that this choice is no severe restriction, since it is deduced from a multipole expansion of the mass distribution. The reduced matrix elements $\langle 1\rangle^m$ to $\langle 5\rangle^m$ were adjusted in the CC analyses to give an optimum description of the measurements (solid lines). The sensitivity of the calculations to these matrix elements is discussed below in the comparison to the data.

For the scattering to the 2_1^+ state the cross section is dominated by the transition strength $|\langle 1\rangle^m|^2$. The analyzing power on the other hand is a relative measurement and therefore nearly independent of $\langle 1\rangle^m$, but highly sensitive to the diagonal element $\langle 2\rangle^m \sim Q_{2_1^+}$, which enters linearly in the interference term of the scattering process. In Fig. 2 the solid and dashed curves for the 2_1^+ excitation show the effect of changing the sign of the quadrupole moment $Q_{2_1^+}$ in the calculations. Both $\sigma(\theta)$ and $iT_{11}(\theta)$ are influenced. Whereas the changes are rather small in $\sigma(\theta)$, they occur in $iT_{11}(\theta)$ as large angular shifts. A destructive interference due to a negative quadrupole moment leads to a shift towards backward angles and to a damping of the diffraction pattern, whereas a positive $Q_{2_1^+}$ results in a forward angle shift and increased oscillations. (In the elastic scattering the interference of the pure potential scattering with the back-coupling term $\langle 1\rangle^m \times\langle 2\rangle^m\langle 1\rangle^m$ also causes angular shifts opposite in direction to those in the inelastic scattering. They are especially pronounced at low projectile energies[8] and decrease considerably with increasing energy.)

In the 2_2^+ scattering, the influence of the quadrupole moment of the 2_2^+ state on the observables is generally much weaker though still significant and its behavior similar to that observed in the 2_1^+ scattering. The effect of the sign change in $Q_{2_2^+}$ is seen in Fig. 2 by comparing corresponding dashed and solid lines for the 2_2^+ excitation. Both $\sigma(\theta)$ and $iT_{11}(\theta)$ are affected distinctively. The main features in this scattering process, however, are caused in general by the P_3 term. This can be seen from the solid and dotted lines in Fig. 2, which show the results of changing the sign of P_3 in the calculations. For all four nuclei the influence of P_3 both on $\sigma(\theta)$ and on $iT_{11}(\theta)$ shows up very clearly and leads to unambiguous assignments for phase and magnitude of P_3. On the contrary, the 2_1^+ scattering of these nuclei is affected only very weakly by P_3 and Q_2 and the drawn curves for the 2_1^+ excitation stay essentially unaltered, if the sign of these are changed.

In Table I we have related the deduced mass matrix elements $\langle f||Q^m||i\rangle$ to electromagnetic quantities by $\langle f||Q^c||i\rangle = (3/4\pi)ZeR_c^2\langle f||Q^m||i\rangle$ using equivalent charge radii R_c from electron scattering[13] and assuming equivalence of mass and charge distributions in the investigated nuclei.

TABLE I. Comparison of electromagnetic properties deduced from this work with results from Coulomb excitation and γ-ray studies. For our results we assume uncertainties of (5–10)% for $B(E2,\, 2_1^+ \rightarrow 0_1^+)$ and of (20–40)% for the other quantitites.

	^{24}Mg		^{28}Si		^{32}S		^{54}Cr	
	This work	Ref. 9	This work	Ref. 10	This work	Ref. 11	This work	Ref. 12
$B(E2,\, 2_1^+ \rightarrow 0_1^+)$[a]	17.2	20.5 ± 0.6	14.3	13 ± 1	10.1	10 ± 1	14.7	13.9 ± 0.5
$B(E2,\, 2_2^+ \rightarrow 0_1^+)$[a]	1.2	1.4 ± 0.3	0.4	0.3 ± 0.1	1.4	1.8 ± 0.4	0.9	...
$B(E2,\, 2_2^+ \rightarrow 2_1^+)$[a]	9.4	2.7 ± 0.4	1.8	2.2 ± 0.6[b]	13.5	12 ± 3	3.2	...
Sign (P_3)	+		−		+		+	
$eQ_{2_1^+}$ ($e\cdot$fm^2)	−14	−27 ± 5[d] −24.3 ± 3.5[d] −24 ± 6[d]	+17	+17 ± 3[c] +17 ± 5[d] +11 ± 5[d]	−13	−12 ± 4[c] −6.6 ± 1.7[d] −17.5 ± 5[d]	−26	−21 ± 8
$eQ_{2_2^+}$ ($e\cdot$fm^2)	+(14)		−(17)		+(13)	20 ± 6[d]	+(26)	

[a]In Weisskopf single-particle units (Ref. 11).
[b]Pure $E2$ assumed.
[c]Ref. 13.
[d]See Ref. 2.

Except for ^{54}Cr all the corresponding $B(E2)$ (Refs. 9-12) and $eQ_{2_1^+}$ (Refs. 2 and 13) values are known from Coulomb excitation and γ-ray studies. Assuming an uncertainty in the determination of the matrix elements of (5–30)% depending on their sensitivity to the data, we get an excellent agreement with the $B(E2)$ values for all nuclei except for the $2_2^+ \rightarrow 2_1^+$ transition in ^{24}Mg, where we obtain a three times bigger $B(E2)$ value which agrees with the model predictions of a static deformed triaxial rotor as well as with microscopic calculations.[14] Use of the much smaller value of Ref. 8 in the calculation leads to a cross section a factor of 2 too small compared with the data. The deduced quadrupole moments agree with results of Coulomb reorientation measurements for ^{54}Cr, ^{32}S, and ^{28}Si, while for ^{24}Mg our value is smaller, but compares favorably with microscopic calculations.[14,15] For ^{32}S there are a number of measurements,[2] which yield small and large $eQ_{2_1^+}$ values. Our intermediate result is in excellent agreement with the most recent published value.[13] Considering the detailed structure of the 2_2^+ scattering data we may also draw conclusions on the quadrupole moment $Q_{2_2^+}$, particularily on its sign, which has not been measured previously and which is extremely important for the test of macroscopic and microscopic[15] models. The absolute values of $Q_{2_2^+}$ given in brackets in Table I are collective-model predictions. Since together with the appropriate signs they give an improved description of the data (solid lines), we consider them to be qualitatively correct. For the phase of P_3 there exists no other measurements to compare with. From our analysis we conclude that for all four nuclei this phase is always opposite to the sign of the quadrupole moment in the 2_1^+ state (solid lines in Fig. 2) resulting, thus, in a negative value for $P_4 = P_3 Q_{2_1^+}$. This is in accord with collective-model predictions[16] as well as with microscopic calculations[14] in the case of the sd-shell nuclei.

In conclusion, our results for the dynamic transition amplitudes and the static moments agree very favorably with microscopic calculations[14] for the sd shell. However, they also support remarkably well simple collective pictures of these nuclei. This points to a pronounced predominance of simple symmetries which characterizes the low-energy spectrum of these nuclei both in its static and in its dynamic properties. A systematic investigation with advanced collective models would be highly desirable.

In this Letter we have demonstrated a strong sensitivity of polarized-deuteron scattering to interference terms in the reaction process. In a systematic analysis of $\sigma(\theta)$ and $iT_{11}(\theta)$, these can be exploited to determine simultaneously signs and magnitudes of both dynamic transition amplitudes and static moments, which supply important information on the structure of nuclei.

This work was supported in part by the Bundesministerium für Forschung und Technologie. One of us (S. T. H.) is a Max Planck Fellow.

(a)On leave from the Institute of Atomic Energy, Pek-

ing, People's Republic of China.
[1]F. Todd Baker, Phys. Rev. Lett. 43, 195 (1979).
[2]C. M. Lederer and V. S. Shirley, *Table of Isotopes* (Wiley, New York, 1978), 7th ed.
[3]H. Clement *et al.*, to be published.
[4]For ^{28}Si the $2_3{}^+$ level could not be separated from the $2_2{}^+$; its contribution is expected to be negligible according to its decay properties [M. A. Meyer, I. Venter, and D. Reitmann, Nucl. Phys. A250, 235 (1975)].
[5]J. Raynal, Saclay, code ECIS, 1974.
[6]J. M. Lohr and W. Haeberli, Nucl. Phys. A232, 381 (1974).
[7]T. Tamura, Rev. Mod. Phys. 37, 679 (1965).
[8]H. Clement, G. Graw, W. Kretschmer, and S. Stach, J. Phys. Soc. Jpn. Suppl. 44, 570 (1978).
[9]D. Branford, A. C. McGough, and I. F. Wright, Nucl. Phys. A241, 349 (1975).
[10]See Meyer, Venter, and Reitmann, Ref. 4.
[11]P. M. Endt and C. van der Leun, Nucl. Data Tables 13, 67 (1974), and Nucl. Phys. A310, 1–752 (1978).
[12]C. W. Towsley, D. Cline, and R. N. Horoschko, Nucl. Phys. A250, 381 (1975).
[13]G. C. Ball, O. Häusser, T. K. Alexander, W. G. Davies, J. S. Forster, and D. Horn, Bull. Am. Phys. Soc. 24, 613 (1979).
[14]W. Knüpfer and J. Stumm, private communication.
[15]I. Morrison, Phys. Lett. 91B, 4 (1980).
[16]K. Kumar, Phys. Lett. 29B, 25 (1969).

Single-Particle Spectra Associated with High-Multiplicity Events in 800-MeV/Nucleon Ar on KCl and Pb

S. Nagamiya, M.-C. Lemaire,[a] S. Schnetzer, H. Steiner, and I. Tanihata[b]
Lawrence Berkeley Laboratory and Department of Physics, University of California, Berkeley, California 94720
(Received 31 March 1980)

High-multiplicity events were selected in collisions of 800-MeV/nucleon Ar on KCl and Pb. In these events, projectile fragments are highly suppressed, and the angular distributions of high-energy protons are almost isotropic in a moving frame whose rapidity is y_0 ($y_0 \simeq 0.60$ for KCl and 0.43 for Pb targets). Comparisons with inclusive proton data are used to estimate the relative importance of single and multiple *NN* collisions. Pion spectra in high-multiplicity events are also presented.

PACS numbers: 25.70.-z

If one describes high-energy heavy-ion collisions in terms of *NN* (nucleon-nucleon) collisions, inclusive particle production would originate from both single *NN* collisions (clean knockout process) and subsequent multiple *NN* collisions (multiple cascade process), because the mean free path of nucleons inside the nucleus[1] is known to be comparable to the typical reaction size of the colliding nuclei.[2,3] In fact, the importance of both processes has been clearly demonstrated in a recent two-proton correlation experiment.[4,5]

High-multiplicity events (hereafter called HME) are events in which a large number of nucleons are actively involved. We thus expect that the detection of HME tends to select small impact parameters and to enhance multiple *NN* collisions. Because several collective phenomena have been predicted for events where multiple *NN* collisions dominate, selecting HME is of special interest. The results reported here focus mainly on high-energy protons and pions in HME, and can be considered to be complementary to those of Stock *et al.*,[6] who measured mainly low-energy protons (≤ 200 MeV).

In order to select HME, we used nine sets of tag-counter telescopes placed at 40° with respect to the beam direction and arranged almost symmetrically in azimuth. Each telescope consisted of two plastic detectors with an absorber sandwiched in between. We selected only high-energy particles, typically $E_{\text{proton}} \geq 100$ MeV, since low-energy protons below 50 MeV could come from target evaporation which is not the type of HME in which we were interested. The solid angle of each telescope was 48 msr which subtended $\Delta\theta = 10°$ and $\Delta\varphi = 22°$. We measured energy and angular distributions of light fragments with a magnetic spectrometer[4] as a function of the particle multiplicity in these telescopes. Typically, spectra of protons between 50 and 2000 MeV were measured by the spectrometer at laboratory angles of 10°–110°.

In order to understand our tag-counter system, especially to study the relationship between the

